Effect of the Ethylene Content of Poly(ethylene-*co*-vinyl alcohol) on the Formation of Microporous Membranes via Thermally Induced Phase Separation

HIDETO MATSUYAMA,[1] KIYOTAKA KOBAYASHI,[1] TAISUKE MAKI,[1] MASAAKI TEARAMOTO,[1] HITOSHI TSURUTA[2]

[1] Department of Chemistry and Materials Technology, Kyoto Institute of Technology, Matsugasaki, Sakyo-ku, Kyoto 606-8585, Japan

[2] Kurashiki Research Laboratory, Kuraray Company, Limited 2045-1, Sakazu, Kurashiki, Okayama 710-8691, Japan

Received 21 September 2000; accepted 26 March 2001

ABSTRACT: Porous poly(ethylene-*co*-vinyl alcohol) (EVOH) membranes were prepared via thermally induced phase separation. The effect of the EVOH ethylene content on the membrane morphology and solute rejection property was investigated. For EVOHs with ethylene contents of 27–44 mol %, polymer crystallization (solid–liquid phase separation) occurred, and the membrane morphology was the particulate structure. However, the liquid–liquid phase separation occurred before crystallization for EVOH with a 60 mol % ethylene content. Cellular pores were formed in this membrane. For the particulate membranes, higher solute rejection and lower water permeance were obtained for EVOH with a lower ethylene content. The membrane formed by the liquid–liquid phase separation showed a sharper solute rejection change with a change in the solute radius than the particulate membranes did. © 2001 John Wiley & Sons, Inc. J Appl Polym Sci 82: 2583–2589, 2001

Key words: poly(ethylene-*co*-vinyl alcohol) membranes; thermally induced phase separation; effect of ethylene content; solute rejection; porous membranes; phase separation

INTRODUCTION

Poly(ethylene-*co*-vinyl alcohol) (EVOH) is a crystalline random copolymer that has good wet strength with hydrophilicity. EVOH has been attracting attention in biomedical fields, especially because of its excellent blood compatibility. Yamashita et al.,[1] Sakurada et al.,[2] and Chen and Young[3] investigated hemodialysis by EVOH membranes and proved the usefulness of EVOH membranes.

Porous EVOH membranes have mainly been prepared by the traditional wet process, that is, the immersion precipitation method. A homogeneous polymer solution is immersed in a nonsolvent bath. The penetration of the nonsolvent into the polymer solution induces phase separation; consequently, a porous structure is formed. Nakamae et al.[4] investigated the effect of the EVOH molecular weight on membrane properties. Membranes prepared from higher molecular weight EVOH had smaller pores and showed lower water fluxes. They discussed the membrane formation mechanism from the viewpoint of the membrane microstructure. Young and coworkers comprehensively studied the EVOH membrane formation mechanism by the immersion precipitation

Correspondence to: H. Matsuyama (matsuyama@chem.kit.ac.jp).

Journal of Applied Polymer Science, Vol. 82, 2583–2589 (2001)

method. They clarified the phase behavior of an EVOH–solvent–nonsolvent system[5] and calculated the diffusion trajectory in the immersion process.[6] Effects attributed to the types of nonsolvents used[7] and solvent evaporation[8] were investigated. Furthermore, solute rejections through several types of EVOH membranes, such as asymmetric and particulate morphologies, were studied.[9] Skinless particulate membranes exhibited not only a high permeation rate with respect to albumin and immunoglobulins but also good selectivity between these components.[10] This means that the particulate EVOH membrane has the potential to be used for treating disorders related to immunoglobulin abnormalities.

An alternative way to produce porous membranes is a thermally induced phase separation (TIPS) process.[11–19] In the TIPS process, a homogeneous polymer solution melt-blended at a high temperature is cooled to induce phase separation. Thus, no nonsolvent is required in the TIPS process. In previous articles, we prepared porous EVOH membranes by the TIPS process.[20] Porous structures were formed by solid–liquid phase separation (polymer crystallization) rather than liquid–liquid phase separation. We controlled crystalline particle sizes by changing the polymer concentration and cooling rate. Permeability was examined with respect to solutes of various sizes.[21] Higher solute rejection and lower water permeance were obtained with increasing polymer concentrations and cooling rates in the TIPS process.

In our previous studies, only one kind of EVOH with a 32 mol % ethylene content (EC) was used. The effect of the EVOH EC on membrane formation by the TIPS process was investigated in this work. The phase diagrams were changed by the EC. In the EVOH with a high EC, liquid–liquid phase separation was observed in addition to solid–liquid phase separation. This change in phase separation led to changes in both the membrane morphology and the solute rejection property.

EXPERIMENTAL

Materials and Characterization of EVOH

Five kinds of EVOHs with different ECs were kindly supplied by Kuraray Co. (Tokyo, Japan). The ECs and degrees of polymerization are summarized in Table I. The degrees of polymerization were not so different in the five EVOHs. The diluent was 1,3-propanediol of an extra-pure reagent grade (Nacalai Tesque Co., Kyoto, Japan).

Table I Properties of EVOH

EC (mol %)	Degree of Polymerization	Contact Angle of Water (°)
27	1000	73
32	1080	76
38	960	80
44	940	85
60	700	88

The contact angles of water on EVOH surfaces are also included in Table I. The contact angle was measured with a contact-angle meter (Kyowa Kaimenkagaku Co., Ltd., Tokyo, Japan, CA-A) at room temperature. In this measurement, a 1-μL water drop was placed on the polymer surface. With an increasing EC, the contact angle increased, which indicated that EVOH became more hydrophobic.

To check the thermal stability of EVOH, we performed a thermogravimetric analysis (TGA) with a Shimadzu TGA-50 (Kyoto, Japan) under a nitrogen atmosphere. The sample was heated from room temperature to 773 K at a heating rate of 20 K/min.

Phase Diagrams

Homogeneous polymer–diluent samples were prepared by a method reported by Kim and Lloyd.[17] A 3–5-mg sample was sealed in an aluminum differential scanning calorimetry (DSC) pan, usually melted at 473 K for 3 min, and then cooled at 10 K/min with a Perkin Elmer DSC-7. The onset of the exothermic peak during the cooling was taken as the dynamic crystallization temperature.

Cloud points were determined with an optical microscope (Olympus, Tokyo, Japan, BX 50). The polymer–diluent sample was placed between a pair of microscope coverslips. To prevent diluent loss by evaporation, we inserted a 100-μm-thick Teflon film with a square opening in the center between the coverslips. The coverslip sample was placed on a hot stage (Linkam, LK-600PH), heated at 473 K for 1 min, and then cooled at a constant rate of 10 K/min with a Linkam L-600A controller. We determined the cloud points visually by noting the appearance of turbidity under the microscope.

Membrane Preparation and Filtration Experiment

Membranes used for the filtration experiment were prepared as follows. The homogeneous polymer–diluent sample was placed between a pair of glass plates (100 mm long, 100 mm wide, and 2.8 mm thick). For adjusting the membrane thickness, a 200-μm-thick Teflon film with a square opening in the center was inserted between the glass plates. Only for a 30 wt % EVOH sample with an EC of 60 mol % was a Teflon film 500 μm thick used because the obtained membrane was not so tight. We heated the glass plates at 413 K in an oven for 15 min to cause melt blending. Then, the glass plates were cooled in air at room temperature. After cooling, the membrane was peeled from the plates and stored in water.

The apparatus and procedure for the filtration experiment were the same as those described previously.[21] The filtration experiment was performed with a stirred cell (Advantec Co., Tokyo, Japan, UHP-25K) at a stirring speed of 1300 rpm. The feed solution was pressurized by nitrogen gas from 0.5 to 3.0 atm. The solutes used were lysozyme from egg white (Seikagaku Co., Tokyo, Japan, 6X crystallized, molecular weight = 14,600, Stokes radius = 1.69 nm[21]), ovalbumin (Sigma Chemical Co., St. Louis, MO, grade V, 98% purity, molecular weight = 45,000, Stokes radius = 2.53 nm[21]), ferritin from horse spleen (Nacalai Tesque, Kyoto, Japan, molecular weight = 440,000, Stokes radius = 6.77 nm[21]), and a polystyrene latex particle (Duke Scientific Co., Palo Alto, CA, radius = 50 nm). The feed solutions were prepared by the dissolution of the proteins in a 0.05 mol/dm^3 phosphate-buffered solution (disodium hydrogenphosphate and potassium dihydrogenphosphate, pH 7.0). The protein concentrations were 0.1 g/dm^3 for lysozyme, 0.2 g/dm^3 for ovalbumin, and 0.002 g/dm^3 for ferritin. The latex particle was dispersed in an aqueous nonionic surfactant (0.01 % Triton X-100) at a concentration of 1.03×10^{11} particles/dm^3. The solute concentrations in the filtrate were measured with a UV spectrophotometer (Hitachi Co., Tokyo, Japan, U-2000) at wavelengths of 280 nm for lysozyme and ovalbumin, 275 nm for ferritin, and 385 nm for the latex particle.

Scanning Electron Microscopy (SEM) Observations

The membranes used for the filtration experiment and the smaller membrane sample prepared with the hot stage were immersed in *t*-butyl alcohol for about 1 day and freeze-dried. The microporous membrane was fractured in liquid nitrogen and mounted vertically on a sample holder. The surface of the sample was sputtered with Au/Pd *in vacuo*. We used a scanning electron microscope (Hitachi Co., S-2300) with an accelerating voltage of 15 kV to examine the membrane cross sections.

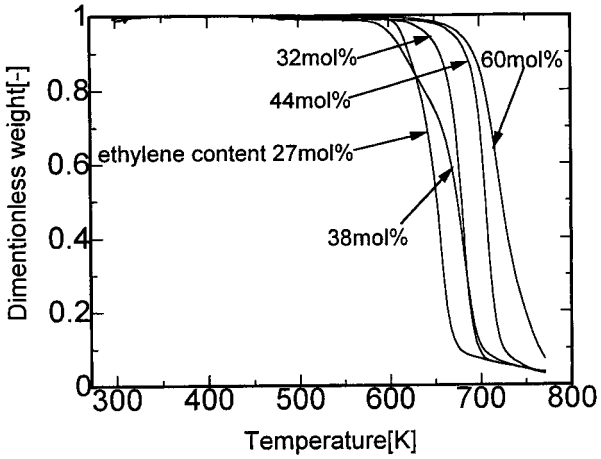

Figure 1 TGA results for EVOH.

RESULTS AND DISCUSSION

Figure 1 shows the TGA results. For all EVOH samples, the dimensionless weight, which is defined as the weight divided by the initial weight, hardly changed up to 573 K. As described previously, the highest temperature used in the TIPS process was 473 K, which is much lower than the temperature at the onset of EVOH pyrolysis shown in Figure 1. Thus, the pyrolysis of EVOH can be ignored in this TIPS process.

Figure 2 shows the phase diagrams for various EVOHs with different ECs. For EVOHs with ECs of 27–44 mol %, the dynamic crystallization temperature approximately agreed with the temperature at which the particle was detected with the optical microscope during cooling, although the latter is not shown in the figure. This means that no structure formation was observed with the microscope at a temperature higher than the dynamic crystallization temperature, and the cloud point, which was the border of the liquid–liquid phase separation, did not exist in the higher temperature region. Therefore, the phase separation during the cooling was a solid–liquid phase separation (polymer crystallization) for these EVOHs. Under the pure polymer condition, the dynamic

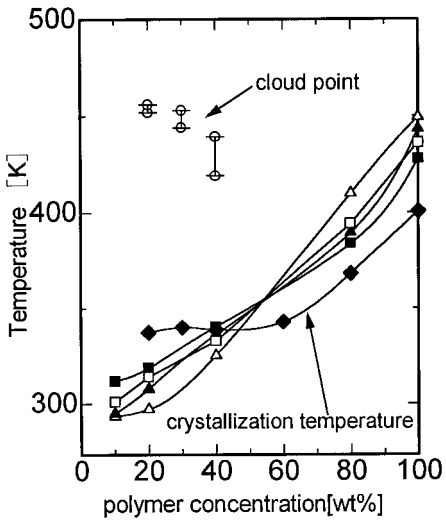

Figure 2 Phase diagram for various EVOHs with different ECs: (△) crystallization temperature, 27 mol % EC; (▲) crystallization temperature, 32 mol % EC; (□) crystallization temperature, 38 mol % EC; (■) crystallization temperature, 44 mol % EC; (◆) crystallization temperature, 60 mol % EC; and (○) cloud point, 60 mol % EC.

crystallization temperature decreased with an EC increase because the melting point of polyethylene (410 K) is lower than that of poly(vinyl alcohol) (505 K).[22] Although the crystallization temperature decreased with the decrease in the polymer weight percentage, the degree of the decrease was influenced by the compatibility between the EVOH and diluent. The solubility parameters for these EVOHs are summarized in Table II. As the EC in EVOH decreased, the solubility parameters approached the diluent value, which indicated that the compatibility became better. When the compatibility was good, the polymer was not likely to crystallize, and the dynamic crystallization temperature decreased. Thus, for EVOH with a lower EC, the degree of the decrease in the crystallization temperature brought about by the decrease in the polymer concentration was higher. Therefore, as shown in Figure 2, the order of the crystallization temperature in the lower polymer concentration region was the opposite of that under the pure polymer condition. Only for EVOH with a 60 mol % EC were cloud points representing the borders of liquid–liquid phase separation observed. As can be expected from the solubility parameters, the compatibility between this EVOH and the diluent was the lowest; it shifted the position of the cloud point to the higher temperature. Thus, the type of phase separation in this EVOH, which was liquid–liquid phase separation, was quite different from the solid–liquid phase separation in other EVOHs.

Table II Solubility Parameters

Substance	Solubility Parameter ($MPa^{1/2}$)
EVOH (27 mol % EC)	23.07[a]
EVOH (32 mol % EC)	22.57[a]
EVOH (38 mol % EC)	21.97[a]
EVOH (44 mol % EC)	21.37[a]
EVOH (60 mol % EC)	19.77[a]
1,3-Propanediol	23.95[b]

[a] Estimated by interpolation from the solubility parameter (15.76 $MPa^{1/2}$) of polyethylene[22] and parameter (25.78 $MPa^{1/2}$) of poly(vinyl alcohol).[22]

[b] Estimated by the use of the group contribution method by Hoy.[23]

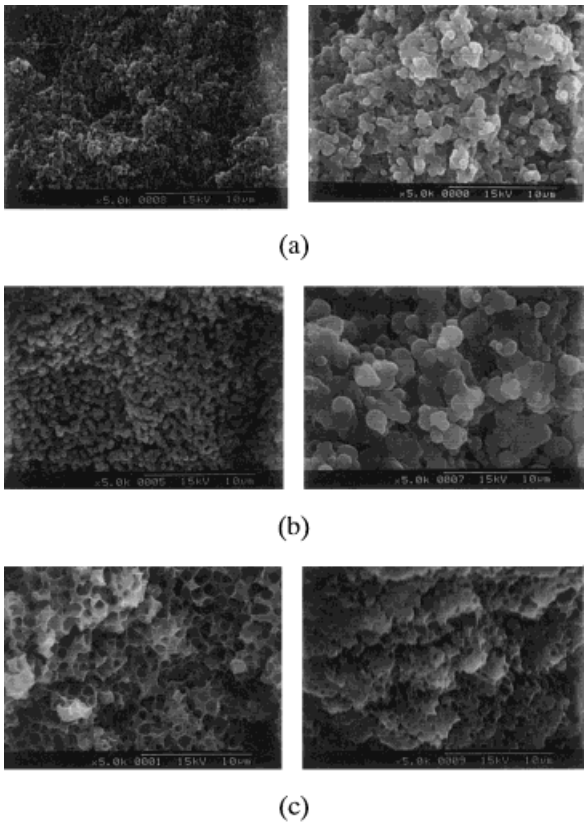

Figure 3 SEM photomicrographs of cross sections of membranes with polymer concentrations of 20 (left) and 40 wt % (right): (a) 32, (b) 44, and (c) 60 mol % EC.

Figure 3 shows SEM photomicrographs of cross sections of the membranes when the polymer solutions were cooled at a rate of 10 K/min with the hot stage. When the ECs of EVOHs were 32 and

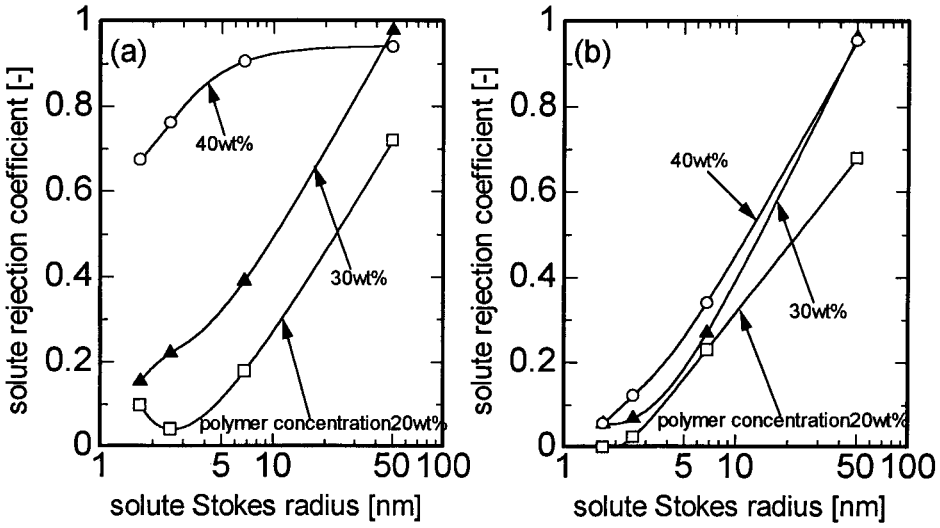

Figure 4 Relation between the apparent solute rejection coefficient and the solute Stokes radius: (a) 32 and (b) 44 mol % EC.

44 mol %, particulate structures were obtained. These structures were attributable to the polymer crystallization expected from the phase diagram shown in Figure 2. The particle size increased with increasing polymer concentration for each EVOH. This tendency is the same as that obtained previously.[20] At the same polymer concentration, EVOH with the higher EC showed a larger particle size. As shown in Figure 2, the dynamic crystallization temperatures were higher for EVOH with a 44 mol % EC than for EVOH with a 32 mol % EC when the polymer concentrations were 20 and 40 wt %. Therefore, for EVOH with a 44 mol % EC, the polymer mobility was higher at the beginning of the crystallization because of the high temperature, and a crystallization period from the onset to cessation of the crystallization at the low temperature was longer if the crystallization was stopped at the same temperature in two EVOHs. This might lead to a larger particle due to higher crystalline growth for EVOH with a 44 mol % EC. However, the membrane of EVOH with a 60 mol % EC showed a cellular pore structure, which indicated the phase-separation type was liquid–liquid phase separation. In this EVOH, the cloud points could be observed at a temperature higher than the crystallization temperature, as shown in Figure 2. Therefore, the liquid–liquid phase separation occurred before crystallization. As the polymer concentration increased from 20 to 40 wt %, the pore size decreased because the higher polymer concentration led to slower pore coarsening because of the higher viscosity of the matrix phase and the lower volume fraction of the pore phase.[24] The result in Figure 3 shows that the membrane structures greatly depended on the EVOH EC.

Figure 4 shows the relations between the apparent solute rejection coefficient and the solute Stokes radius when the polymer concentrations were changed. The apparent solute rejection coefficient R is defined as

$$R = 1 - C_f/C_0 \tag{1}$$

where C_0 and C_f are solute concentrations in the feed and filtrate, respectively. For EVOHs with 32 and 44 mol % ECs, the rejection coefficient increased with the increase in the polymer concentration. The solute permeated through these particulate membranes via interconnected open pores between particles. As the polymer concentration increased, the membrane porosity decreased,[21] which meant that the open pores between the particles became small. This is the reason for the increase in the rejection coefficient. The degree of the increase in R is more remarkable for EVOH with a 32 mol % EC than for EVOH with a 44 mol % EC. The reason for this tendency is not clear.

The effects of the EVOH EC on the rejection coefficient are shown in Figure 5. EVOH with a 32 mol % EC showed a higher rejection coefficient than EVOH with a 44 mol % EC for two polymer

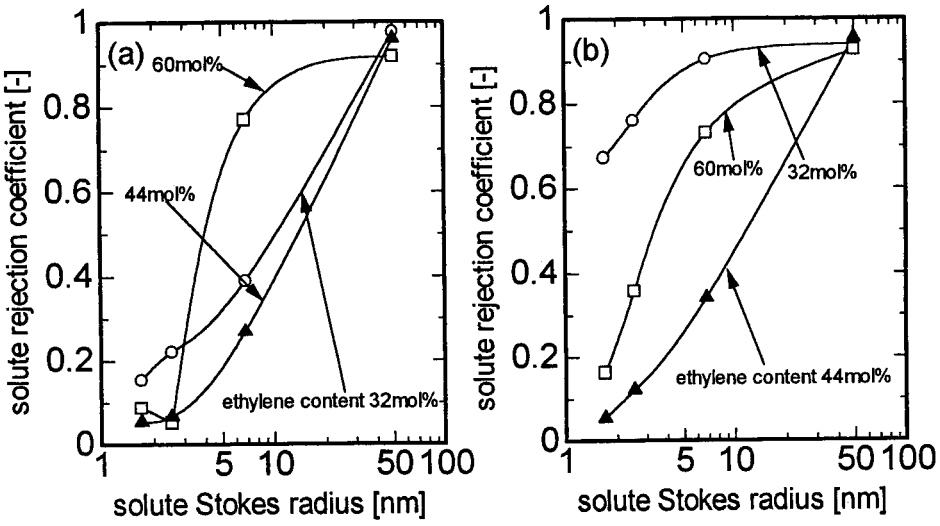

Figure 5 Effect of the EVOH EC on the rejection coefficient: (a) 30 and (b) 40 wt % polymer concentration.

concentrations. When the polymer concentrations were the same, the porosities of the obtained membranes could be expected to be similar. Thus, the difference in the rejection coefficient was not attributable to the difference in the membrane porosity. The structures of the membranes used for the filtration experiments were similar to those shown in Figure 2. Therefore, the EVOH membrane with a 32 mol % EC had a smaller particle size. The smaller particle led to smaller channels of open pores between particles. This contributed to an increase in the rejection coefficient. The membranes of EVOH with a 60 mol % EC, which were formed by liquid–liquid phase separation, showed relatively sharper rejection changes with changes in the solute sizes. This may indicate a sharper pore size distribution in this membrane compared with that in the membranes formed by polymer crystallization.

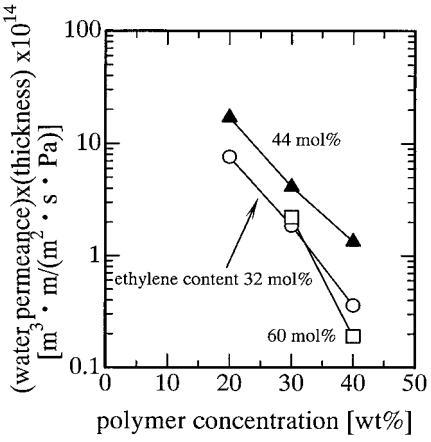

Figure 6 Relation between the pure water permeance and the polymer concentration.

Figure 6 shows the relation between the pure water permeance and the polymer concentration. The water permeance is defined as the volumetric flow rate divided by the membrane area and pressure difference. The ordinate of this figure is a permeance multiplied by the membrane thickness to correct the difference in the membrane thickness. The water permeance decreased with an increase in the polymer concentration because of the decrease in the membrane porosity. EVOH with a 44 mol % EC showed higher water permeance than EVOH with a 32 mol % EC. As shown in Figure 2, the former membrane had a larger particle size, which led to a larger channel size. This is the reason for the higher water permeance. The membrane of EVOH with a 60 mol % EC, which was formed by liquid–liquid phase separation, showed a lower water permeance, probably because of the poor connection of pores, as shown especially for a polymer concentration of 40 wt % in Figure 3(c).

CONCLUSION

Phase diagrams for EVOH with various ECs were obtained. For EVOHs with ECs of 27–44 mol %, polymer crystallization occurred during the cooling process. In the low polymer concentration re-

gion, the dynamic crystallization temperatures decreased with a decrease in the EC, whereas the opposite tendency was obtained in the high polymer concentration region. Only for EVOH with a 60 mol % EC were cloud points, defined as the borders of liquid–liquid phase separation, were observed.

EVOHs with ECs of 32 and 44 mol % showed crystalline particle structures. The particle size was larger for EVOH with the higher EC. However, the cellular pores were formed by liquid–liquid phase separation in EVOH with a 60 mol % EC.

The solute rejections were investigated. As the polymer concentration increased, the membranes of the particulate structure showed a high solute rejection coefficient with a lower water permeance. The higher rejection coefficient and lower water permeance were obtained with the EVOH EC decreasing. A membrane with cellular pores showed a relatively sharp rejection change with a change in the solute size.

REFERENCES

1. Yamashita, S.; Nagata, S.; Takakura, K. Kobunshi Ronbunshu 1979, 36, 249.
2. Sakurada, Y.; Sueoka, A.; Kawahashi, M. Polym J 1987, 19, 501.
3. Chen, L.-W.; Young, T. H. Makromol Chem Macromol Symp 1990, 33, 183.
4. Matsumoto, T.; Nakamae, K.; Ochiumi, T.; Horie, S. J Membr Sci 1981, 9, 109.
5. Young, T.-H.; Lai, J.-Y.; You, W.-M.; Cheng, L.-P. J Membr Sci 1997, 128, 55.
6. Cheng, L.-P.; Young, T.-H.; You, W.-M. J Membr Sci 1998, 145, 77.
7. Young, T.-H.; Hsieh, C.-C.; Chen, L.-Y.; Huang, Y.-S. J Membr Sci 1999, 159, 21.
8. Young, T.-H.; Huang, Y.-H.; Chen, L.-Y. J Membr Sci 2000, 164, 111.
9. Cheng, L.-P.; Lin, H.-Y.; Chen, L.-W.; Young, T.-H. Polymer 1998, 39, 2135.
10. Lin, D.-T.; Cheng, L.-P.; Kang, Y.-J.; Chen, L.-W.; Young, T.-H. J Membr Sci 1998, 140, 185.
11. Castro, A. J. U.S. Pat. 4,247,498 (1981).
12. Caneba, G. T.; Soong, D. S. Macromolecules 1985, 18, 2538.
13. Hiatt, W. C.; Vitzthum, G. H.; Wagener, K. B.; Gerlach, K.; Josefiak, C. In Microporous Membranes via Upper Critical Temperature Phase Separation; Lloyd, D. R., Ed.; ACS Symposium Series 269; American Chemical Society: Washington, DC, 1985; p 229.
14. Lloyd, D. R.; Kinzer, K. E.; Tseng, H. S. J Membr Sci 1990, 52, 239.
15. Tsai, F.-J.; Torkelson, J. M. Macromolecules 1990, 23, 775.
16. Lloyd, D. R.; Kim, S.-S.; Kinzer, K. E. J Membr Sci 1991, 64, 1.
17. Kim, S.-S.; Lloyd, D. R. J Membr Sci 1991, 64, 13.
18. Vadalia, H. C.; Lee, H. K.; Myerson, A. S.; Levon, K. J Membr Sci 1994, 89, 37.
19. Mehta, R. H.; Madsen, D. A.; Kalika, D. S. J Membr Sci 1995, 107, 93.
20. Matsuyama, H.; Iwatani, T.; Kitamura, Y.; Teramoto, M.; Sugo, N. J Appl Polym Sci 2001, 79, 2449.
21. Matsuyama, H.; Iwatani, T.; Kitamura, Y.; Teramoto, M.; Sugo, N. J Appl Polym Sci 2001, 79, 2456.
22. Brandrup, J.; Immergut, E. H. Polymer Handbook, 3rd ed.; Wiley: New York, 1989.
23. Hoy, K. L. J Paint Technol 1970, 46, 76.
24. Matsuyama, H.; Berghmans, S.; Lloyd, D. R. Polymer 1999, 40, 2289.